Małgorzata I. MICHALCZYK*

ACTIVE NOISE CONTROL WITH MOVING ERROR MICROPHONE

SUMMARY

Electro-acoustic plants controlled by active noise control (ANC) systems in enclosures are usually time-varying. Their changes can be caused by movements of an error microphone, around which zones of quiet are created. Then, the time variations of the electro-acoustic plant can be fast and adaptive ANC algorithms for tracking variations of error microphone position should be used. The preliminary research results showed that the created zone of quiet can move tracking the movement of the error microphone, when filtered-x least mean squares (FX-LMS) algorithm is applied. The paper presents further results of real-world experiments conducted on a special laboratory stand, which enabled to move the error microphone round the circle trajectory with constant rotational speed.

Two modifications of FX-LMS algorithm were applied in order to accelerate control algorithm convergence and improve tracking properties of the ANC system: normalized FX-LMS and modified FX-LMS algorithm. It was shown, that the zone of quiet can track movement of the error microphone, however, there was no significant difference in control algorithms performance. In all cases the zone of quiet tracked the movement of the error microphone, even for the error microphone velocity as high as 3.7 m/s, and high attenuation was obtained – from 16 dB for the fast microphone movement up to 28 dB for the slowest microphone movement.

Keywords*: adaptive control, acoustic noise, feedforward systems, LMS algorithm*

UKŁAD AKTYWNEGO TŁUMIENIA HAŁASU Z PORUSZAJĄCYM SIĘ MIKROFONEM BŁĘDU

Obiekty elektroakustyczne w układach aktywnego tłumienia hałasu (ATH) są zazwyczaj zmienne w czasie. Ich zmiany mogą być spowodowane m.in. ruchem mikrofonu błędu, wokół którego tworzone są przestrzenne strefy ciszy. Zastosowanie adaptacyjnych algorytmów ATH do śledzenia szybkich zmian pozycji mikrofonu błędu jest słabo zbadane. Wstępne badania pokazały, że strefa ciszy może poruszać się za mikrofonem błędu, w przypadku gdy algorytmem sterowania jest algorytm LMS z filtracją sygnału odniesienia (FX-LMS). Artykuł prezentuje wyniki badań w układzie ATH na specjalnym stanowisku laboratoryjnym umożliwiającym ruch mikrofonu po okręgu z zadaną szybkością.

Aby zwiększyć szybkość zbieżności algorytmu FX-LMS, zastosowano dwie jego literaturowe modyfikacje: znormalizowany algorytm FX-LMS i zmodyfikowany algorytm FX-LMS. Pokazano, że strefa ciszy nadąża za ruchem mikrofonu, jednak nie ma znaczącej różnicy pomiędzy działaniem układu z zastosowaniem poszczególnych badanych algorytmów. We wszystkich przypadkach, strefa ciszy śledziła mikrofon, nawet dla ruchu z prędkością linową 3,7 m/s, i uzyskano wysokie tłumienie zakłócenia – od 16 dB dla największej prędkości mikrofonu do 28 dB w przypadku wolnego ruchu mikrofonu.

Słowa kluczowe*: sterowanie adaptacyjne, hałas, systemy predykcyjne, algorytmy LMS*

1. INTRODUCTION

Electro-acoustic plants controlled by active noise control (ANC) systems in enclosures are usually time-varying. Some of variations are caused by changes of air temperature and humidity or movements of objects and persons in an enclosure. To deal with these variations adaptive control algorithms are applied, what is widely described in the literature (Kuo *et al*. 1996). Sometimes there is a need to assure low noise level around a moving user. Then, the time variations of the electro-acoustic plant can be fast, as the person equipped with the error microphone can move quickly. In such situation adaptive ANC algorithms for tracking of fast variations of error microphone position should be used. Some preliminary research results presented in (Błażej *et al*. 2001; Czyż 2007; Michalczyk 2004, 2005; Michalczyk *et al*. 2006) show, that the created zone of quiet can move tracking the movement of the error microphone, when filtered-x least mean squares (FX-LMS) algorithm is used. The behaviour of the zone of quiet was experimentally observed and it was shown in (Michalczyk *et al.* 2006), how the tracking properties depend on the step size.

The research on ANC with moving microphone is a specific task. Generally, adaptive control algorithms are used for initial calculation of controller coefficients and to deal with slow changes of an electro-acoustic plant. For such tasks the adaptation is set to be slow. When the ANC system is tracking moving error microphone adaptive control algorithm has to be parameterised in a different way – the adaptation is set to be fast enough to track the movements of the error microphone. However, the limits of the step size μ of FX-LMS algorithm assuring convergence of the adaptive control algorithm were determined using slow convergence assumption. Thus the choice of step size is a very difficult task.

* Institute of Automatic Control, Silesian University of Technology, Gliwice; e-mail: malgorzata.michalczyk@polsl.pl

The paper presents the results of real-world experiments concerning the behaviour of the ANC system with moving error microphone for different adaptive control algorithms tested to improve system performance.

2. ACTIVE NOISE CONTROL SYSTEM

The ANC system presented in this paper is used to create 3-dimensional zones of quiet in enclosure of cubature of 70 m^3 (Fig. 1). It is the one-channel adaptive system of feedforward structure with reference microphone (M_x in Fig. 1). The zone of quiet is created around the error microphone M_e (Figs 1–2) that picks up the error signal. Two channels of the electro-acoustic plant can be defined: a secondary path, including electronic instrumentation and an acoustic part of the enclosure between the control loudspeaker and the error microphone, denoted $S(z^{-1})$, and the acoustic feedback path.

2.1. Laboratory stand

In order to evaluate the influence of a movement of the error microphone on the ANC system performance a special laboratory stand was build (Fig. 2) (Michalczyk *et al*. 2006). It enables to move the error microphone round the circle trajectory with constant or variable rotational speed. Four observation microphones – M_1, M_2, M_3 and M_4 – are located around the circle (Fig. 2), about 3 cm over the trajectory of the error microphone.

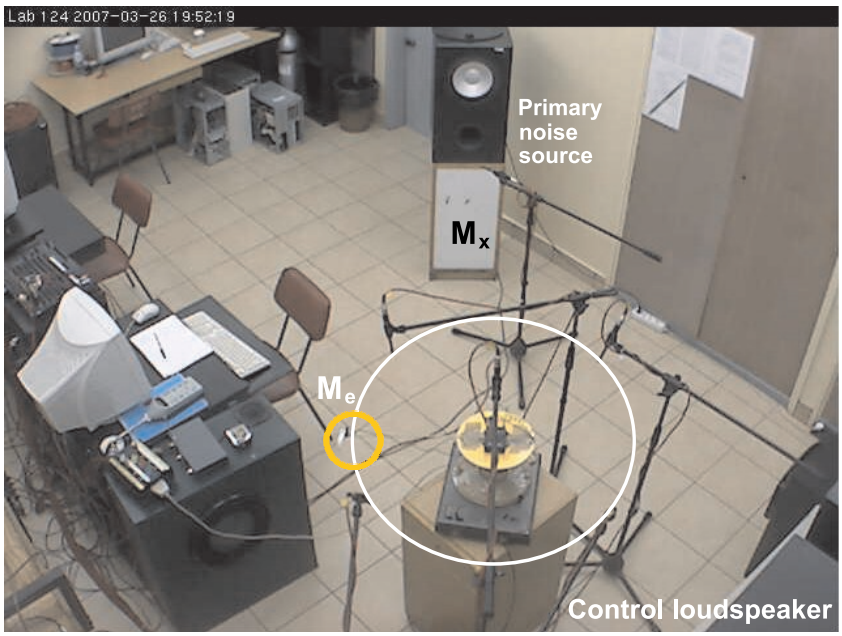

Fig. 1. ANC system for creation of 3D zones of quiet in enclosure

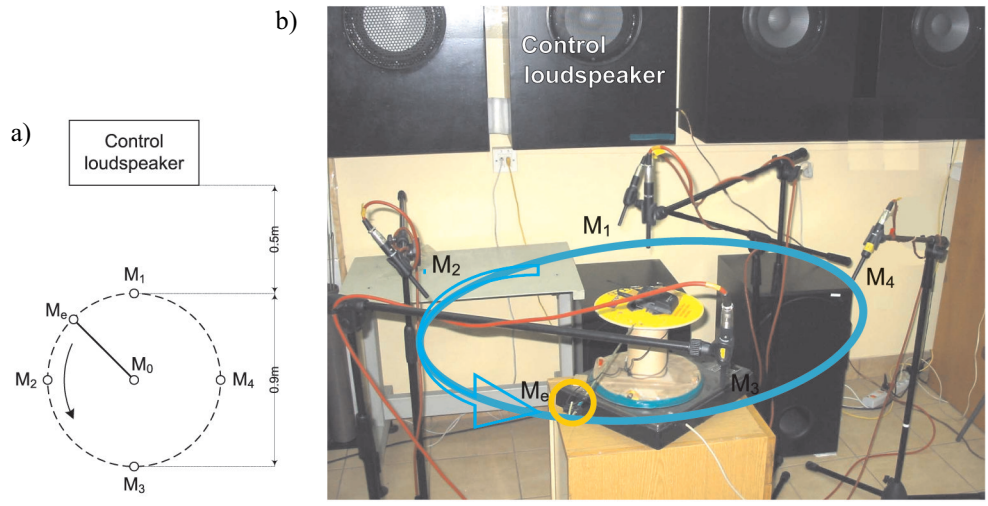

Fig. 2. The laboratory stand enabling the movement of the error microphone and the observation microphones positions: a) scheme; b) photo (error microphone trajectory denoted with cyan circle)

The observation microphones are used to pick up the signals, that along with the error microphone signal are sampled with frequency of 10 kHz and recorded using dSPACE DS1104 Board. Using the recorded data the disturbance attenuation in all microphones was calculated.

The rotational speed can range from about 0.2 to 1.3 rotations per second. In the experiments presented in this paper the diameter of the circle was set on 0.9 m, thus the linear velocity of the error microphone ranged from 0.5 to 3.7 m/s.

2.2. Electro-acoustic plant

The electro-acoustic plant controlled by the ANC system includes electronic elements and an acoustic space. The acoustic space can change very significantly causing a large change of electro-acoustic plant dynamic properties, especially if it is the inside of an enclosure. The strongest nonstationarities are caused by movements of the error microphone in the enclosure, causing huge changes in the secondary path dynamics, both changes of the phase and the magnitude. The increase of the phase estimation error, if exceeds $\pm\pi/2$, results in divergence of the adaptive control algorithm (Kuo *et al*. 1996). The change of the magnitude of the secondary path may also result in control algorithm divergence, if the step size is too large. If the spatial range of such nonstationarity is small, i.e. generated by small (in comparison with the disturbance wavelength) dislocations of the error microphone it was shown that this kind of nonstationarities can be dealt with the use of standard adaptive control algorithm. The preliminary experiments that gave promising results were reported in (Błażej *et al*. 2001; Czyż 2007; Michalczyk 2004, 2005; Michalczyk *et al.* 2006). Severe nonstationarities of a wide spatial range can be generated by large dislocations of the error microphone or by significant changes of the secondary path dynamics. In such case the electro-acoustic plant models should be additionally identified *on-line* (Kuo *et al*. 1996; Michalczyk 2004), however, it makes adaptation process much more complicated.

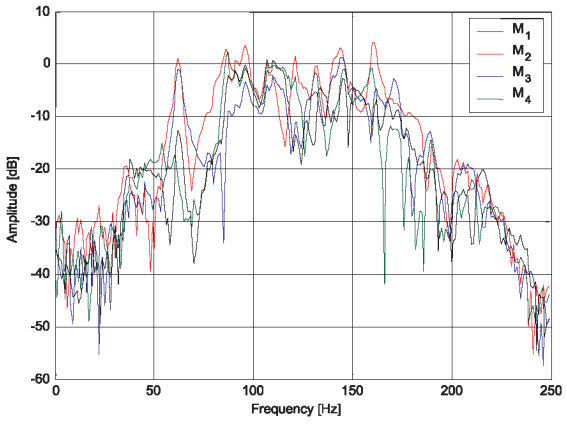

Fig. 3. Magnitude of the frequency response of the secondary path for the error microphone M_e located in M_1, M_2, M_3 and M_4 observation positions

The frequency responses of the secondary path for four locations of the error microphone are shown in Figure 3. It can be seen that for some frequencies there are large variations in magnitude. It is imposed by complicated dynamics of the reverberant enclosure. It is extremely difficult to parameterise the standard adaptive control algorithm, choosing step size value for large variations in magnitude. However, for some frequencies the variations are smaller, e.g. a few decibels of a difference in magnitude and negligible variations in phase for frequency 96 Hz. The variations in phase are smaller, because the length of the noise wave was large in comparison to the circle diameter. Thus, the periodic disturbance of frequency 96 Hz (the pure tone) was chosen for experiments.

2.3. Adaptive control algorithms

The adaptive controller is applied, employing FX-LMS algorithm (Kuo *et al.* 1996) and its modifications, all with neutralisation of acoustic feedback (Kuo *et al*. 1996; Michalczyk 2004). The identification of electro-acoustic plant models necessary for parameterisation of the control algorithm is performed before the activation of the ANC system (Michalczyk 2004) with the error microphone located in position M_1 (Fig. 2) in the distance of about 0.5 m from the control loudspeaker. The controller FIR filter order was $N = 2$ and step size μ was chosen experimentally. The control algorithm was implemented in TMS320C31 Texas Instruments DSP on dSPACE DS1102 Board. The sampling frequency was equal 500 Hz.

The FX-LMS algorithm is the most popularly used for adaptation of controller coefficients in ANC systems. The block diagram of the exemplary system is shown in Figure 4. A short description of this algorithm is given below, for details see (Kuo *et al.* 1996).

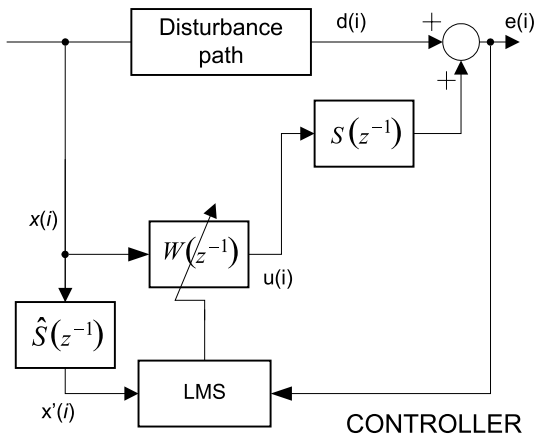

Fig. 4. 'Filtered-x' ANC system structure

A reference microphone picks up a reference signal $x(i)$ filtered to obtain control signal

$$u(i)=\boldsymbol{x}^{\mathrm{T}}(i)\boldsymbol{w}(i) \tag{1}$$

where:

$\boldsymbol{x}(i)=\left[x(i),x(i\text{-}1),\ldots,x(i\text{-}N+1)\right]^{\mathrm{T}}$ – vector of delayed reference signal values $x(i)$,

$\boldsymbol{w}(i)=\left[w_0(i),w_1(i),\ldots,w_{N-1}(i)\right]^{\mathrm{T}}$ – vector of $W(z^{-1})$ FIR controller filter coefficients

N – controller filter order.

The controller filter coefficients are updated at every time instant i according to

$$\boldsymbol{w}(i+1)=\boldsymbol{w}(i)-\mu e(i)\boldsymbol{x}'(i) \tag{2}$$

where:

$$e(i)=d(i)+S\left(z^{-1}\right)u(i) \tag{3}$$

– error signal measured by an error microphone,

$d(i)$ – disturbance signal that should be attenuated,

$\boldsymbol{x}'(i)=\left[x'(i),x'(i\text{-}1),\ldots,x'(i\text{-}N+1)\right]^{\mathrm{T}}$ – vector of filtered reference signal values, obtained by the filtration

$$x'(i)=\hat{S}\left(z^{-1}\right)x(i) \tag{4}$$

using a model $\hat{S}\left(z^{-1}\right)$ of the secondary path transfer function $S\left(z^{-1}\right)$.

A constant μ is the step size controlling the convergence of the algorithm. To assure FX-LMS algorithm convergence in the case of perfect modeling of the secondary path $\left(\hat{S}\left(z^{-1}\right)=S\left(z^{-1}\right)\right)$ the step size μ should be chosen from the range

$$0<\mu<\frac{2}{P_{x'}(N+1)} \tag{5}$$

where $P_{x'}=\mathrm{E}\left\{\left(x'(i)\right)^2\right\}$ is an estimate of the power of the filtered reference signal $x'(i)$.

Two FX-LMS algorithm modifications were implemented for tests: normalised FX-LMS (NFX-LMS) algorithm (Kuo *et al.* 1996) and modified FX-LMS (MFX-LMS) algorithm (Bjarnason 1992; Rupp *et al*. 1998). Both were designed to improve poor convergence of FX-LMS algorithm. In NFX-LMS algorithm the step size is weighted by the power of filtered reference signal (picked up by the reference microphone M_x). For MFX-LMS algorithm the error signal is modified to neutralise the influence of the secondary path dynamics (Bjarnason 1992; Rupp *et al*. 1998).

The choice of the step size μ is independent of the reference signal properties, if the following normalisation of the FX-LMS algorithm is applied:

$$\boldsymbol{w}(i+1)=\boldsymbol{w}(i)-\mu(i)\hat{\boldsymbol{x}}'(i)e(i) \tag{6}$$

where the step size $\mu(i)$ is time dependent

$$\mu(i)=\frac{\alpha}{\hat{\boldsymbol{x}}'^{\mathrm{T}}(i)\hat{\boldsymbol{x}}'(i)} \tag{7}$$

and α is a positive constant. This algorithm is called NFX-LMS algorithm. Since $\hat{\boldsymbol{x}}'^{\mathrm{T}}(i)\hat{\boldsymbol{x}}'(i)$ is an estimate of $P_{x'}(N+1)$ in (5), the constant α for the NFX-LMS algorithm should be chosen within the range $0<\alpha\le 2$.

The poor speed of convergence of FX-LMS algorithm is caused by the delay existing in the secondary path. Bjarnasson (1992) suggested a system modification that removes is delay – MFX-LMS algorithm (Fig. 5). An error signal $\varepsilon(i)$ used for adaptation of controller filter coefficients is calculated using error signal $e(i)$, control signal $u(i)$ filtered through the secondary path model and signal $x(i)$ filtered through the controller filter $W\left(z^{-1}\right)$. In the case of perfect modeling of the secondary path $\left(\hat{S}\left(z^{-1}\right)=S\left(z^{-1}\right)\right)$ the value of $e'(i)$ represents disturbance signal $d(i)$ and the delay introduced by the secondary path is thoroughly removed.

In ANC systems used to create 3D zones of quiet a reference microphone is used and an acoustic feedback occurs between a control loudspeaker and this microphone. Since acoustic feedback can destabilise the system (Kuo *et al.* 1996) the neutralisation of this phenomenon is applied by filtration of control signal $u(i)$ using a model of the acoustic feedback path. Consequently, two electro-acoustic plant models are necessary for the ANC system activation.

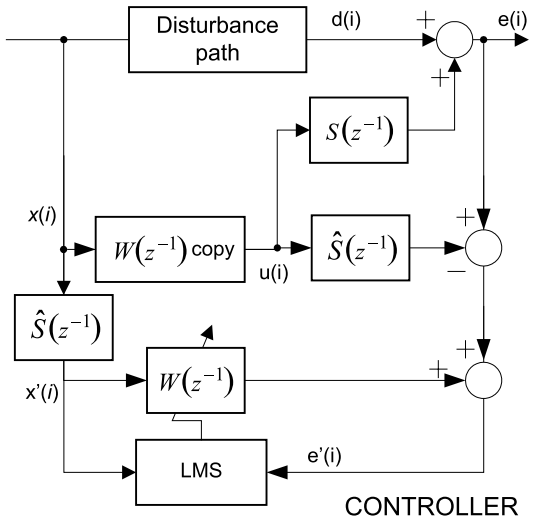

Fig. 5. Modified 'filtered-x' ANC system structure

3. RESULTS OF REAL-WORLD EXPERIMENTS

A large number of real-world experiments were conducted to observe the behaviour of the ANC system with moving error microphone. The linear velocity of the error microphone was set to the values: v = 0.5, 2.1 and 3.7 m/s. Step size values were chosen dependently on the adaptive control algorithm used correspondingly for FX-LMS algorithm μ about 0.12, α for NFX-LMS about 0.1 and μ = 1.0 for MFX-LMS algorithm unless otherwise stated.

For nonstationary conditions (moving error microphone) the disturbance attenuation was calculated in the following way:

$$J(i) = J(iT) = -10\log_{10}\left(\frac{\hat{\sigma}'^2_e(i)}{\hat{\sigma}'^2_d(i)}\right) \tag{8}$$

where the estimate of the variance $\hat{\sigma}'^2_e(i)$ of the error signal $e(i)$ was calculated for the ANC system activated in two steps. The first was the calculation of the error signal power with exponential smoothing with experimentally chosen smoothing factor α = 0.997. The second step was the additional smoothing of the obtained error signal power $\hat{\sigma}^2_e(i)$ estimate using moving average $\hat{\sigma}'^2_e(i) = MA\left\{\hat{\sigma}^2_e(i)\right\}$ with the window length N_{MA} = 48. Disturbance signal $d(i)$ power estimate $\hat{\sigma}'^2_d(i)$ was calculated in the same way. All measurements were taken after the initial adaptation stage.

3.1. Stationary conditions

For stationary conditions (no movement of the error microphone) the noise attenuation was measured using sound level meter using linear scale (its microphone was kept a few centimetres from the error microphone). The disturbance of the frequency 96 Hz is attenuated to the background noise level. If the error microphone is located in the position M_1 the attenuation near the observation microphones is correspondingly about 35 dB in M_1, about 29 dB in M_2 and about 30 dB both in M_3 and M_4.

3.2. Movement of the zone of quiet

In Figure 6 the attenuation $J(i)$ in the observation microphone M_1 is shown as a function of time, corresponding to the error microphone position, for the linear velocity v = 3.7 m/s. Four attenuation $J(i)$ curves were obtained with step size values μ = 0.0001, 0.01, 0.1 and 0.15. It can be noticed that almost constant attenuation $J(i)$ =11 dB is observed for the lowest step size value. For larger μ value the attenuation $J(i)$ slightly oscillates around 12 dB level. For μ = 0.1 the zone of quiet starts to track the error microphone – attenuation changes from 6 to over 22 dB. The maximum attenuation is obtained about 100 ms after the error microphone goes through the position M_1. It means that the zone of quiet tracks the error microphone, but is delayed. For the highest value of the step size μ = 0.15 attenuation changes from 4 to 25 dB. Now, the highest attenuation is obtained only 50 ms after the moment the error microphone goes through the observation position. It means, that the zone of quiet moves with the error microphone, surrounding it.

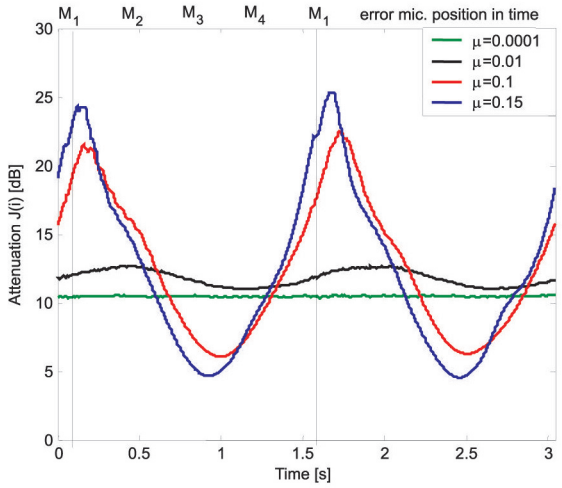

Fig. 6. Attenuation $J(i)$ in observation microphone M_1 for v = 3.7 m/s and for different values of μ for FX-LMS algorithm

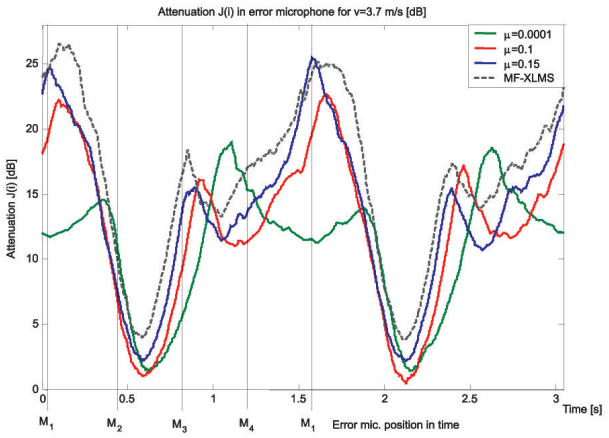

Fig. 7. Attenuation $J(i)$ in error microphone M_e for v = 3.7 m/s and for different values of μ for FX-LMS algorithm and for MFX-LMS algorithm

The attenuation $J(i)$ in error microphone recorded in the next experiment is shown in Figure 7. As it is known for stationary plant and was shown in (Michalczyk *et al.* 2006) for a nonstationary plant, generally the larger value of the step size of the adaptive control algorithm, the higher is the obtained attenuation in error microphone. It is especially visible when the error microphone approaches the position M_3 – then the attenuation growth is proportional to step size. The disturbance signal power $\hat{\sigma}'^2_d(i)$ recorded for the error microphone velocity v = 3.7 m/s shown in Figure 8 explains, why the very low attenuation is obtained for error microphone position between M_2 and M_3 observation microphones. The disturbance signal power to the background noise power ratio is very low in that region, thus only low attenuation level can be obtained.

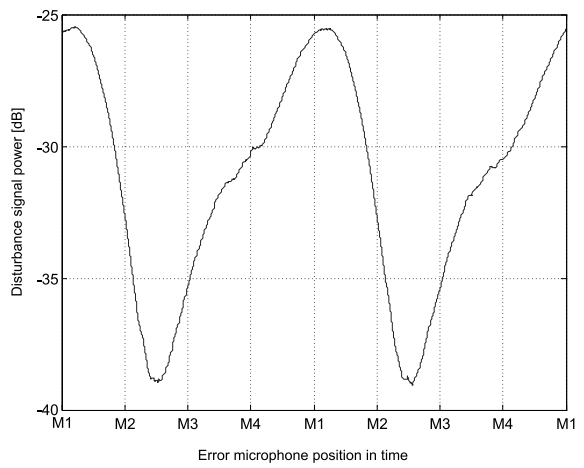

Fig. 8. Disturbance signal power $10\log_{10}\left(\hat{\sigma}'^2_d(i)\right)$ recorded for v = 3.7m/s

There was shown in (Michalczyk *et al*. 2006) that the increasing intensity of the movement deteriorates the ANC system performance. This can be illustrated by the attenuation $J(i)$ curves (Fig. 9) in function of the error microphone position changing in normalised time. The disturbance attenuation was picked up by the error microphone for three values of the error microphone velocity: v = 0.5, 2.1 and 3.7 m/s. The highest attenuation is obtained in the ANC system for the slowest error microphone movement. When the error microphone velocity is increased, the attenuation is lower and it is increasingly more difficult for the adaptive control algorithm to follow quickly changing conditions.

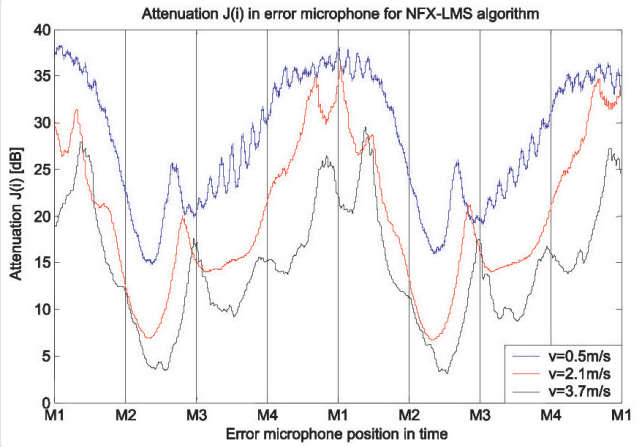

Fig. 9. Attenuation $J(i)$ in error microphone M_e for different values of microphone velocity for NFX-LMS algorithm

3.3. Performance of different adaptive control algorithms

Two modifications of FX-LMS algorithm were applied in order to accelerate control algorithm convergence and improve tracking properties of the ANC system with moving error microphone. It was shown in (Rupp *et al*. 1998) that for the stationary plant the MFX-LMS algorithm is characterized by much faster convergence than the FX-LMS algorithm. It is also known (Kuo *et al*. 1996), that NFX-LMS algorithm is characterized by faster convergence than FX-LMS algorithm. The same conclusions were drawn from observations of the initial adaptation stage (controller coefficients set to zero). The MFX-LMS algorithm obtained the final attenuation level almost at once, NFX-LMS algorithm was slower and it took a longer time for FX-LMS to adapt controller coefficients.

However, results of experiments showed, that after initial adaptation stage, only slight difference in performance of these algorithms can be observed. The results shown in Figure 10 were obtained for the discussed algorithms with the step size chosen individually in experimental way to assure best performance of the ANC system. The NFX-LMS algorithm turned out to be characterised by the fastest convergence for the nonstationary electro-acoustic plant. MFX-LMS algorithm gave slightly higher attenuation, however was slightly slower. FX-LMS algorithm assured also slightly worse performance of the ANC system than the previous algorithms.

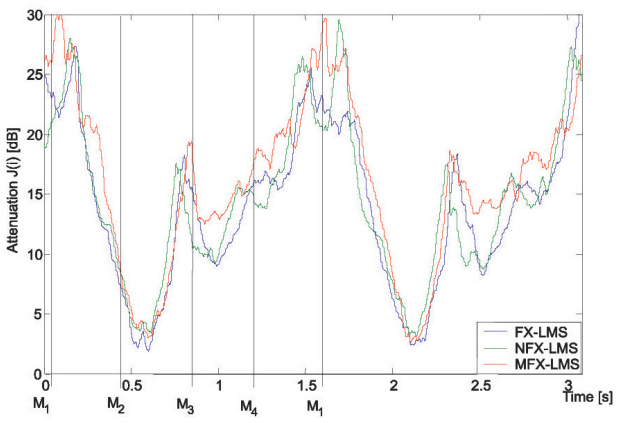

Fig. 10. Attenuation $J(i)$ in error microphone M_e for different control algorithms, v = 3.7m/s

The mean attenuation in the error microphone calculated over two rotations is shown in the Table 1. Again, the difference in attenuation is slight. MFX-LMS algorithm allows to obtain the larger attenuation. It is worth to notice, that this algorithm is much more sensitive on step size choice.

Table 1. Mean attenuation in M_e over two rotations [dB]

Adaptive control algorithm	v=0.5m/s	v=2.1m/s	v=3.7m/s
FX-LMS	28	19	14
NFX-LMS	28	20	15
MFX-LMS	29	20	16

4. CONCLUDING REMARKS

The ANC system creating zone of quiet around moving error microphone was presented. It was shown that it depends

on adaptation algorithm parameterization how the zone of quiet can track the movement of the error microphone. Well known FX-LMS algorithm modifications were applied to improve ANC system performance. It turned out however, that there is no significant difference in their performance. In all cases the zone of quiet tracked the movement of the error microphone, even for the error microphone velocity as high as 3.7 m/s, and high attenuation was obtained – from 16 dB for the fast microphone movement up to 28 dB for the slowest microphone movement.

Acknowledgements

A partial financial support of this research by Polish Ministry of Science and Higher Education is gratefully acknowledged.

References

Bjarnason E. 1992, *Active noise cancellation using a modified form of the filtered-X LMS algorithm.* Proc. Eusipco-92, Sig. Proc. VI, Belgium, vol. 2, pp. 1053–1056.

Błażej M., Ogonowski Z. 2001, *Non-stationarity of 3-D Zones of Quiet* (in Polish). XLVIII Otwarte Seminarium Akustyki OSA 2001, pp. 197–202.

Czyż K. 2007, *Adaptive Control for Nonstationary Electro-Acoustic Plant.* Materials of The 13th IEEE Int. Conf. on Methods and Models in Automation and Robotics, Szczecin.

Kuo S.M., Morgan D.R. 1996, *Active Noise Control Systems*. *Algorithms and DSP Implementations.* J. Wiley & Sons, N. York, ISBN 0-471-13424-4.

Michalczyk M.I. 2004, *Adaptive control algorithms for three-dimensional zones of quiet*. Skalmierski Computer Studio, Gliwice, ISBN 83-89105-67-5.

Michalczyk M.I. 2005, *Adaptive control algorithms for three-dimensional zones of quiet*. Archives of Control Sciences, Vol. 15, No 1, pp. 53–82.

Michalczyk M.I., Czyż K. 2006, *Active Noise Control with Moving Error Microphone: Preliminary Results*. 13th International Congress on Sound and Vibration, CD-ROM version, Vienna, Austria.

Rupp M., Sayed A.H. 1998, *Robust FxLMS Algorithms with Improved Convergence Performance*. IEEE Transactions on Speech and Audio Processing, 6(1), pp. 78–85.